Published in final edited form as:
Cell Rep. 2012 November 29; 2(5): 1137–1142. doi:10.1016/j.celrep.2012.10.001.

Targeting of XJB-5-131 to mitochondria suppresses oxidative DNA damage and motor decline in a mouse model of Huntington's disease

Zhiyin Xun[1], **Sulay Rivera-Sanchez**[2], **Sylvette Ayala-Peñ**[2,3], **James Lim**[1], **Helen Budworth**[1], **Erin M. Skoda**[4], **Paul D. Robbins**[5], **Laura J. Niedernhofer**[5,6], **Peter Wipf**[4], and **Cynthia T. McMurray**[1,*]

[1]Life Sciences Division, Lawrence Berkeley National Laboratory, Berkeley, CA, 94720 USA

[2]Department of Biochemistry, University of Puerto Rico Medical Sciences Campus, San Juan, PR 00936-5067

[3]Department of Pharmacology and Toxicology, University of Puerto Rico Medical Sciences Campus, San Juan, PR 00936-5067

[4]Department of Chemistry, University of Pittsburgh, Pittsburgh, PA, 15232 USA

[5]Department of Microbiology and Molecular Genetics, University of Pittsburgh, Pittsburgh, PA, 15232 USA

[6]University of Pittsburgh Cancer Institute, University of Pittsburgh, Pittsburgh, PA, 15232 USA

SUMMARY

Oxidative damage and mitochondrial dysfunction are implicated in aging and age-related neurodegenerative diseases, including Huntington's disease (HD). Many naturally occurring antioxidants have been tested to correct for deleterious effects of reactive oxygen species, but often they lack specificity, are tissue variable, and the efficacy is marginal in human clinical trials. To increase specificity and efficacy, we have designed a synthetic antioxidant, XJB-5-131, to target mitochondria. We demonstrate in a mouse model of HD that XJB-5-131 has remarkably beneficial effects. XJB-5-131 reduces oxidative damage to mitochondrial DNA, maintains mitochondrial DNA copy number, suppresses motor decline and weight loss, enhances neuronal survival, and improves mitochondrial function. The findings poise XJB-5-131 as a promising therapeutic compound.

INTRODUCTION

Defective mitochondria (MT) are implicated in the pathogenesis of neurodegenerative diseases including Alzheimer's disease (AD) (Huang and Mucke, 2012), Parkinson's disease (PD) (Exner et al., 2012), and Huntington's disease (HD) (Johri and Beal, 2011). In all of

*Address correspondence to: Cynthia T. McMurray, Life Sciences Division, Lawrence Berkeley National Laboratory, Berkeley, CA 94720, USA. Phone: 510-486-6526; Fax: 510-486-6880; ctmcmurray@lbl.gov.

CONFLICT OF INTEREST

The authors have declared that no conflict of interest exists.

these disorders, accumulation of oxidative damage is involved (Exner et al., 2012; Huang and Mucke, 2012; Johri et al., 2011), but there are no effective therapeutics (Hersch and Rosas, 2008; Mangialasche et al., 2010). MT are the primary intracellular source of reactive oxygen species (ROS) and the main target for oxidative damage (Lin and Beal, 2006). Thus, dietary supplements of naturally occurring antioxidants such as vitamin E and coenzyme Q_{10} (CoQ_{10}) have been used in mice and in human clinical trials to alleviate the deleterious effects of MT-dependent ROS production (Dumont et al., 2011; Littarru and Tiano, 2010). In general, however, their efficacy has been marginal or tissue variable (Kwong et al., 2002; Sohal and Forster, 2007; Sumien et al., 2009), and it remains controversial whether dietary supplementation of CoQ_{10} can increase its steady-state level in the brain *in vivo* (Kwong et al., 2002; Sohal and Forster, 2007). These observations have driven efforts to enhance specificity and therapeutic efficacy by direct targeting of synthetic antioxidants to MT.

XJB-5-131 is a bi-functional antioxidant that comprises a radical scavenger, 4-hydroxy-2,2,6,6-tetramethyl piperidine-1-oxyl nitroxide (Figure 1A, **red**) conjugated to a mitochondrial targeting moiety. The targeting portion of the molecule is an alkene peptide isostere modification of the Leu-D-Phe-Pro-Val-Orn segment of the antibiotic, gramicidin S (Hoye et al., 2008; Wipf et al., 2005) (Figure 1A, **black**) that localizes to the mitochondrial membrane. Previously, we have reported that XJB-5-131 reduces apoptosis and enhances cell survival in mouse embryonic cells *in vitro* (Wipf et al., 2005). In this work, we tested the beneficial effects of XJB-5-131 in a mouse model of HD. We find that XJB-5-131 significantly suppresses the disease phenotypes and improves mitochondrial function.

RESULTS

XJB-5-131 is localized to MT and improves primary neuronal survival

We evaluated the efficacy of XJB-5-131 in a mouse model of HD harboring disease-length 150 CAG tract "knocked-into" both alleles of the mouse HD gene homologue (*Hdh*$^{(CAG)150/(CAG)150}$) (Lin et al., 2001). These animals will be referred to hereafter as *HD150KI*. To validate that XJB-5-131 targeted MT, we isolated primary striatal neurons (embryonic day 17) from *HD150KI* animals and treated them with BODIPY-FL-XJB-5-131, a derivative of XJB-5-131 labeled with the fluorescent (FL) boron-dipyrromethene (BODIPY) (Figure 1A). Within one hour of incubation, BODIPY-FL-XJB-5-131 crossed the plasma membrane and stained MT in primary neurons, as verified by co-staining with MitoTracker Deep Red (Figure 1B). Treatment of freshly plated primary neurons with XJB-5-131 (1 μM) for 7 days did not induce measureable changes in the number of MT (Figure 1C). However, under these conditions, XJB-5-131 improved survival of the primary striatal neuronal cultures derived from both *HD150KI* mice (Figure 1D) and genetically matched C57BL/6 wild type mice (Figure S1), suggesting that accumulation of XJB-5-131 in the MT was beneficial to the primary neuronal cultures *in vitro*.

XJB-5-131 suppresses weight loss and improves motor performance

We tested whether XJB-5-131 had beneficial effects *in vivo*. We intraperitoneally injected *HD150KI* mice with XJB-5-131 at 1 mg/kg three times a week up to 57 weeks, and tested whether treatment improved the disease phenotypes in these animals. Chronic treatment of *HD150KI* mice with XJB-5-131 suppressed weight loss, a pathology commonly observed in HD patients (Kirkwood et al., 2001). Genetically matched C57BL/6 control animals increased in weight to an average of 44 ± 5 g at 57 weeks (Figure 2A), while age- and gender-matched *HD150KI* mice were smaller (32 ± 3 g) (Figure 2A). Treatment of *HD150KI* animals with XJB-5-131 increased the average body mass by 22% (Figure 2A).

Early signs of HD pathology manifest as motor abnormalities (Kirkwood et al., 2001). As a second test for XJB-5-131's efficacy, we measured rotarod performance and grip strength of animals at 9, 28, and 57 weeks (Figure 2B). All animals at 9 weeks performed equally well on the rotarod (Figure 2B). However, performance in *HD150KI* mice declined with age, resulting in an approximately 70% decrease by 57 weeks (Figure 2B). Remarkably, there was no significant decline in rotarod performance in *HD150KI* mice chronically treated with XJB-5-131 during the same period (Figure 2B). Furthermore, XJB-5-131 treatment led to a striking improvement in grip strength (Figure 2C). At 57 weeks, approximately 95% of the *HD150KI* mice failed to grip the bar for 30 seconds in three trials, while at the same age, 85% of the XJB-5-131-treated *HD150KI* littermates passed the test. Collectively, these data demonstrated that XJB-5-131 significantly reduced the disease phenotypes observed in *HD150KI* mice.

XJB-5-131 reduces mtDNA damage and maintains mtDNA copy number

MT are the primary intracellular source of ROS and the main target for oxidative damage (Lin and Beal, 2006; Woo and Shadel, 2011). If the beneficial effects of XJB-5-131 in MT were due to its antioxidant properties *in vivo,* then we anticipated that a reduction in oxidative damage to mtDNA would accompany the improvement in motor function. To test the hypothesis, we applied quantitative PCR (qPCR) to measure whether XJB-5-131 altered the level of oxidative damage to mtDNA. Because the movement of the polymerase on the template is blocked at a lesion, qPCR amplification is inversely proportional to the presence of DNA damage. *HD150KI* animals had a remarkable increase in the load of oxidative mtDNA damage relative to age-matched controls (Figures 3A and 3C). However, treatment with XJB-5-131 led to a reduction in the damage burden (Figures 3A and 3C). Similarly, the abundance of mtDNA molecules in *HD150KI* animals decreased by 36% relative to controls (Figures 3B and 3D), consistent with previous suggestions that mitochondrial biogenesis is impaired in HD animals (Johri et al., 2012). Chronic treatment with XJB-5-131 restored the mtDNA abundance to control levels (Figures 3B and 3D). Thus, XJB-5-131 treatment not only decreased the lesion load in mtDNA but also prevented a decline in the relative abundance of mtDNA in treated *HD150KI* animals relative to untreated littermates (Figures 3A-3D).

XJB-5-131 improves mitochondrial function

Because XJB-5-131 is a MT-targeted antioxidant, we tested its effects on mitochondrial function. MT generate most of the cell's supply of ATP via the oxidative phosphorylation pathway, which is measured by the oxygen consumption rate (OCR) (Zhang et al., 2012). To determine the effects of XJB-5-131 on OCR, we isolated synaptosomes from 57-week *HD150KI* animals and compared OCR before and after treatment with inhibitors of the electron transport chain (Figure 4A). Synaptosomes are "pinched off" nerve terminals that harbor intact neuronal MT and represent a simple and robust system to assess mitochondrial function within a physiological milieu (Choi et al., 2009). Treatment of synaptosomes with 200 nM XJB-5-131 did not induce a measureable change in the relative OCR of resting synaptosomes from *HD150KI* animals (Figure 4B). Similarly, XJB-5-131 had little effect on the relative decrease in OCR in *HD150KI* synaptosomes after inhibition of ATP synthase with oligomycin (Figure 4B). These results implied that XJB-5-131 had minimal effects on mitochondrial metabolism in the resting state. However, XJB-5-131 significantly improved mitochondrial response to cellular stress as measured by the mitochondrial membrane potential uncoupler, fluoro-carbonyl cyanide phenylhydrazone (FCCP) (Figure 4B). FCCP destroys the proton gradient in MT (Figure 4A) and uncouples electron transport from ATP generation. Under these conditions, OCR rises as the MT try to "keep up" with the energy demands of the cell. The rise in OCR after FCCP treatment reflects the maximum ability of MT to maintain energy production in response to acute and chronic stress (Dranka et al.,

2010), and is referred to as mitochondrial spare respiratory capacity (SRC) or reserve capacity (Figure S2). Indeed, treatment of striatal synaptosomes with 1 μM and 10 μM solutions of XJB-5-131 elevated the mitochondrial SRC, as measured by the approximately 2-fold increase in OCR relative to untreated striatal synaptosomes (Figure 4C). XJB-5-131 treatment conferred a similar increase (2-3 fold) on the mitochondrial SRC in *HD150KI* cortical synaptosomes (Figure S2) and in striatal synaptosomes isolated from genetically matched C57BL/6 wild type mice (Figure S2), indicating that the improvement in the mitochondrial stress response was neither limited to the striatum nor specific for the HD mouse model.

XJB-5-131 protects against 2,3-dimethoxy-1,4-naphthoquinone (DMNQ)-induced loss of mitochondrial SRC

XJB-5-131 was designed as a targeted antioxidant. Thus, we tested whether the protective effect of XJB-5-131 against ROS-induced damage was due, at least in part, to the radical scavenging activity of the compound. The ROS-inducer, DMNQ is a non-thiol-capturing and non-alkylating redox cycling quinone that causes continuous intracellular generation of H_2O_2 and subsequent oxidative damage to MT (Figure 4D) (Parry et al., 2009). If XJB-5-131 was a radical scavenger, then we anticipated that it would protect against DMNQ-induced mitochondrial damage and would alter the OCR in synaptosomes in response to DMNQ exposure. As expected, treatment with oligomycin and FCCP increased OCR in synaptosomes from 57-week *HD150KI* animals (Figure 4E). Addition of DMNQ, under these conditions, reduced the SRC (Figure 4E), while administration of XJB-5-131 and DMNQ together recovered the mitochondrial SRC to 90% of control (Figure 4F). The XJB-5-131–induced increase in mitochondrial SRC was robust since subsequent addition of rotenone and antinomycin A, inhibitors of complex I and complex III (Figure 4E), respectively, eliminated OCR differences among treatment groups. These results suggested that the beneficial effects of XJB-5-131 were due, at least in part, to its radical scavenging activity, as designed.

DISCUSSION

Generic and naturally occurring antioxidants have been largely ineffective against neurodegenerative diseases, although mitochondrial dysfunction has been strongly implicated as part of the toxic mechanism (Johri and Beal, 2011; Mangialasche et al., 2010). Here we demonstrate that a synthetic, MT-targeted XJB-5-131 imparts a remarkable suppression of motor decline, inhibits weight loss, reduces mtDNA damage, maintains mtDNA copy number, improves mitochondrial function, and enhances neuronal survival in a knock-in mouse model of HD. Collectively, these findings imply that specific targeting of this synthetic antioxidant to MT has beneficial effects both *in vitro* and *in vivo*, and poise XJB-5-131 as a promising therapeutic compound.

XJB-5-131 has attractive properties. First, its delivery to MT does not depend on the potential gradient across the inner mitochondrial membrane. Rather, selective localization of XJB-5-131 is accomplished via insertion of the β-turn motif within the Leu-D-Phe-Pro-Val-Orn segment into the mitochondrial membrane (Fink et al., 2007). Thus, compromised MT with reduced membrane potential would not exclude entry of XJB-5-131. Indeed, we demonstrate that XJB-5-131 significantly improves mitochondrial function upon the treatment with the membrane potential uncoupler FCCP. This is in contrast to potential-dependent delivery of MT-targeted antioxidants. For example, MitoQ and MitoVit E protect against glutathione depletion in cultured fibroblasts from Friedrich's ataxia patients, yet their enhanced potency is abolished in cells pretreated with FCCP (Jauslin et al., 2003). Moreover, the uptake of these potential-dependent antioxidants is self-limiting, as there is inevitable depolarization of MT upon accumulation of large amounts of cations in the matrix

(Kelso et al., 2001; Smith et al., 1999). Second, XJB-5-131 readily crosses the plasma membrane while exogenously supplemented vitamin E and CoQ_{10} are more lipophilic and tend to be retained in cell membranes. Thus, these naturally occurring compounds have difficulty in achieving pharmacologically significant intracellular concentrations (Jauslin et al., 2003; Szeto, 2006).

XJB-5-131 not only enhances mitochondrial SRC but also protects against DMNQ-induced loss of mitochondrial SRC. Mitochondrial SRC is critical for survival and function of cells, especially under conditions where cells undergo increased oxidative stress or a sudden increase in energy demand (Desler et al., 2012). For example, enhanced mitochondrial SRC favors T cell survival after infection (van der Windt et al., 2012) and loss of mitochondrial SRC renders cell death in the rotenone model of PD with partial Complex I deficiency (Yadava and Nicholls, 2007). In our experiments, the favorable properties of MT-targeted XJB-5-131 suppressed pathophysiology without obvious toxicity. Collectively, the beneficial effects of XJB-5-11 are promising, and warrant further investigations for its efficacy in a broader set of MT-associated disorders and premature aging phenotypes.

EXPERIMENTAL PROCEDURES

More detailed experimental procedures are provided in the Supplemental Information.

Animals

We used a mouse model of HD (Lin et al., 2001), referred to as *HD150KI* mice. Genetically matched C57BL/6 mice were used as controls unless otherwise stated. All procedures involving animals were performed in accordance with the National Institutes of Health Guide for the Care and Use of Laboratory Animals. Protocols were approved by the Lawrence Berkeley National Laboratories Animal Welfare and Research Committee.

XJB-5-131 synthesis, treatment, and assessment of motor functions

XJB-5-131 was synthesized as described previously (Wipf et al., 2005). A Fluorescent (FL) boron-dipyrromethene (BODIPY)-labeled XJB-5-131 was prepared in an analogous fashion. *HD150KI* mice were intraperitoneally injected 1 mg/kg of XJB-5-131 or phosphate buffered saline three times per week from 7 to 57 weeks. Animals in each group (10 for XJB-5-131 treatment group and 7 for untreatment group) were evaluated for rotarod performance and grip strength at 9, 28, and 57 weeks on a Rota-Rod apparatus (Ugo Basile, Italy) according to a protocol described previously_ENREF_3 (Trushina et al., 2006). See Supplemental Information for details.

Culture of primary striatal neurons, MitoTracker Deep Red and BODIPY-FL-XJB-5-131 labeling, and confocal microscopy

Striatal neurons isolated on embryonic day 17 from *HD150KI* mice were cultivated as described elsewhere (Trushina et al., 2004). MitoTracker Deep Red (Invitrogen, Carlsbad, CA) and BODIPY-FL-XJB-5-131 were used to label MT in live primary striatal neurons. Images were acquired on a Zeiss LSM 710 inverted laser scanning confocal microscope. Image J and FIJI was used for image analysis and quantification of cells. See Supplemental Information for details.

Analysis of mtDNA damage and relative abundance by quantitative PCR (qPCR)

The amplification of a 10 kb and a 116 bp mtDNA fragment was used to detect lesions and abundance in mouse cerebral cortex as previously described (Ayala-Torres et al., 2000; Santos et al., 2006). See Supplemental Information for details.

Preparation of striatal and cortical synaptosomes

Striatal and cortical synaptosomes were isolated as previously described (Choi et al., 2009). Protein concentration was determined using the Bio-Rad Bradford assay (BioRad Laboratories). See Supplemental Information for details.

Respiration of synaptic MT

Respiration of synaptic MT was measured by the oxygen consumption rate (OCR) using a Seahorse XF96 Extracellular Flux Analyzer (Seahorse Bioscience, Billerica, MA) according to the manufacturer's instructions. See Supplemental Information for details.

Induction of ROS with 2,3-Dimethoxy-1,4-Naphthoquinone (DMNQ)

Freshly isolated synaptosomes were exposed to 1 μM DMNQ either in the absence or presence of 10 μM XJB-5-131. Synaptosomes were plated on the Seahorse PS 96-well microplate and spun down for 50 minutes at 4°C. The DMNQ exposure time was approximately 90 minutes before the OCR was measured.

Statistical analysis

Values were expressed as mean ± standard error of the mean (SEM), unless otherwise stated. P-values were obtained from the unpaired two-tailed Student's t-test.

Supplementary Material

Refer to Web version on PubMed Central for supplementary material.

Acknowledgments

This work was supported by the National Institutes of Health grants NS40738 (to CTM), GM066359 (to CTM), NS062384 (to CTM), NS060115 (to CTM), CA092584 (to CTM), GM067082 (to PW), AI068021 (to PW), AG024827 (to PDR), AR051456 (to PDR), ES016114 (to LJN), CA103730 (to LJN), the Ellison Medical Foundation (AG-NS-0303-05) (to LJN), and the University of Puerto Rico infrastructural grant (2G12-RR003051) (to EFR).

REFERENCES

Ayala-Torres, S.; Chen, Y.; Svoboda, T.; Rosenblatt, J.; Van Houten, B. Analysis of gene-specific DNA damage and repair using quantitative PCR. In: Doetchst, P., editor. Methods: A Companion to Methods in Enzymology. New York: Academic Press; 2000. p. 135-147.

Choi SW, Gerencser AA, Nicholls DG. Bioenergetic analysis of isolated cerebrocortical nerve terminals on a microgram scale: spare respiratory capacity and stochastic mitochondrial failure. J. Neurochem. 2009; 109:1179–1191. [PubMed: 19519782]

Desler C, Hansen TL, Frederiksen JB, Marcker ML, Singh KK, Juel Rasmussen L. Is There a Link between Mitochondrial Reserve Respiratory Capacity and Aging? J. Aging Res. 2012

Dranka BP, Hill BG, Darley-Usmar VM. Mitochondrial reserve capacity in endothelial cells: The impact of nitric oxide and reactive oxygen species. Free Radic. Biol. Med. 2010; 48:905–914. [PubMed: 20093177]

Dumont M, Kipiani K, Yu F, Wille E, Katz M, Calingasan NY, Gouras GK, Lin MT, Beal MF. Coenzyme Q10 Decreases Amyloid Pathology and Improves Behavior in a Transgenic Mouse Model of Alzheimer's Disease. J. Alzheimers Dis. 2011; 27:211–223. [PubMed: 21799249]

Exner N, Lutz AK, Haass C, Winklhofer KF. Mitochondrial dysfunction in Parkinson's disease: molecular mechanisms and pathophysiological consequences. EMBO J. 2012; 31:3038–3062. [PubMed: 22735187]

Fink MP, Macias CA, Xiao J, Tyurina YY, Jiang J, Belikova N, Delude RL, Greenberger JS, Kagan VE, Wipf P. Hemigramicidin-TEMPO conjugates: novel mitochondria-targeted anti-oxidants. Biochem. Pharmacol. 2007; 74:801–809. [PubMed: 17601494]

Hersch SM, Rosas HD. Neuroprotection for Huntington's disease: ready, set, slow. Neurotherapeutics. 2008; 5:226–236. [PubMed: 18394565]

Hoye AT, Davoren JE, Wipf P, Fink MP, Kagan VE. Targeting mitochondria. Acc. Chem. Res. 2008; 41:87–97. [PubMed: 18193822]

Huang Y, Mucke L. Alzheimer mechanisms and therapeutic strategies. Cell. 2012; 148:1204–1222. [PubMed: 22424230]

Jauslin ML, Meier T, Smith RAJ, Murphy MP. Mitochondria-targeted antioxidants protect Friedreich Ataxia fibroblasts from endogenous oxidative stress more effectively than untargeted antioxidants. FASEB J. 2003; 17:1972–1974. [PubMed: 12923074]

Johri A, Beal MF. Antioxidants in Huntington's disease. BBA-Mol. Basis Dis. 2011

Johri A, Calingasan NY, Hennessey TM, Sharma A, Yang L, Wille E, Chandra A, Beal MF. Pharmacologic activation of mitochondrial biogenesis exerts widespread beneficial effects in a transgenic mouse model of Huntington's disease. Hum. Mol. Genet. 2012; 21:1124–1137. [PubMed: 22095692]

Johri A, Chaturvedi RK, Beal MF. Hugging tight in Huntington's. Nat. Med. 2011; 17:245–246. [PubMed: 21383715]

Kelso GF, Porteous CM, Coulter CV, Hughes G, Porteous WK, Ledgerwood EC, Smith RAJ, Murphy MP. Selective targeting of a redox-active ubiquinone to mitochondria within cells. J. Biol. Chem. 2001; 276:4588–4596. [PubMed: 11092892]

Kirkwood SC, Su JL, Conneally PM, Foroud T. Progression of symptoms in the early and middle stages of Huntington disease. Arch. Neurol. 2001; 58:273. [PubMed: 11176966]

Kwong LK, Kamzalov S, Rebrin I, Bayne ACV, Jana CK, Morris P, Forster MJ, Sohal RS. Effects of coenzyme Q10 administration on its tissue concentrations, mitochondrial oxidant generation, and oxidative stress in the rat. Free Radic. Biol. Med. 2002; 33:627–638. [PubMed: 12208349]

Lin CH, Tallaksen-Greene S, Chien WM, Cearley JA, Jackson WS, Crouse AB, Ren S, Li XJ, Albin RL, Detloff PJ. Neurological abnormalities in a knock-in mouse model of Huntington's disease. Hum. Mol. Genet. 2001; 10:137–144. [PubMed: 11152661]

Lin MT, Beal MF. Mitochondrial dysfunction and oxidative stress in neurodegenerative diseases. Nature. 2006; 443:787–795. [PubMed: 17051205]

Littarru GP, Tiano L. Clinical aspects of coenzyme Q10: an update. Nutrition. 2010; 26:250–254. [PubMed: 19932599]

Mangialasche F, Solomon A, Winblad B, Mecocci P, Kivipelto M. Alzheimer's disease: clinical trials and drug development. Lancet Neurol. 2010; 9:702–716. [PubMed: 20610346]

Parry JD, Pointon AV, Lutz U, Teichert F, Charlwood JK, Chan PH, Athersuch TJ, Taylor EL, Singh R, Luo JL. Pivotal Role for Two Electron Reduction in 2-3-Dimethoxy-1, 4-naphthoquinone and 2-Methyl-1, 4-naphthoquinone Metabolism and Kinetics in Vivo That Prevents Liver Redox Stress. Chem. Res. Toxicol. 2009; 22:717–725. [PubMed: 19338340]

Santos JH, Meyer JN, Mandavilli BS, Van Houten B. Quantitative PCR-based measurement of nuclear and mitochondrial DNA damage and repair in mammalian cells. Methods Mol. Biol. 2006:183–199. [PubMed: 16673882]

Smith RAJ, Porteous CM, Coulter CV, Murphy MP. Selective targeting of an antioxidant to mitochondria. Eur. J. Biochem. 1999; 263:709–716. [PubMed: 10469134]

Sohal RS, Forster MJ. Coenzyme Q, oxidative stress and aging. Mitochondrion. 2007; 7:S103–S111. [PubMed: 17482528]

Sumien N, Heinrich KR, Shetty RA, Sohal RS, Forster MJ. Prolonged intake of coenzyme Q10 impairs cognitive functions in mice. J. Nutr. 2009; 139:1926–1932. [PubMed: 19710165]

Szeto HH. Mitochondria-targeted peptide antioxidants: novel neuroprotective agents. AAPS J. 2006; 8:521–531.

Trushina E, Du Charme J, Parisi J, McMurray CT. Neurological abnormalities in caveolin-1 knock out mice. Behav. Brain Res. 2006; 172:24–32. [PubMed: 16750274]

Trushina E, Dyer RB, Badger JD II, Ure D, Eide L, Tran DD, Vrieze BT, Legendre-Guillemin V, McPherson PS, Mandavilli BS. Mutant huntingtin impairs axonal trafficking in mammalian neurons in vivo and in vitro. Mol. Cell. Biol. 2004; 24:8195–8209. [PubMed: 15340079]

van der Windt GJ, Everts B, Chang CH, Curtis JD, Freitas TC, Amiel E, Pearce EJ, Pearce EL. Mitochondrial respiratory capacity is a critical regulator of CD8+ T cell memory development. Immunity. 2012; 36:68–78. [PubMed: 22206904]

Wipf P, Xiao J, Jiang J, Belikova NA, Tyurin VA, Fink MP, Kagan VE. Mitochondrial targeting of selective electron scavengers: synthesis and biological analysis of hemigramicidin-TEMPO conjugates. J. Am. Chem. Soc. 2005; 127:12460–12461. [PubMed: 16144372]

Woo DK, Shadel GS. Mitochondrial stress signals revise an old aging theory. Cell. 2011; 144:11–12. [PubMed: 21215364]

Yadava N, Nicholls DG. Spare respiratory capacity rather than oxidative stress regulates glutamate excitotoxicity after partial respiratory inhibition of mitochondrial complex I with rotenone. J. Neurosci. 2007; 27:7310–7317. [PubMed: 17611283]

Zhang J, Nuebel E, Wisidagama DRR, Setoguchi K, Hong JS, Van Horn CM, Imam SS, Vergnes L, Malone CS, Koehler CM, et al. Measuring energy metabolism in cultured cells, including human pluripotent stem cells and differentiated cells. Nat. Protoc. 2012; 7:1068–1085. [PubMed: 22576106]

Highlights

- XJB-5-131 suppresses motor decline and weight loss
- XJB-5-131 reduces mtDNA damage and maintains mtDNA copy number
- XJB-5-131 improves mitochondrial function
- XJB-5-131 enhances primary neuronal survival

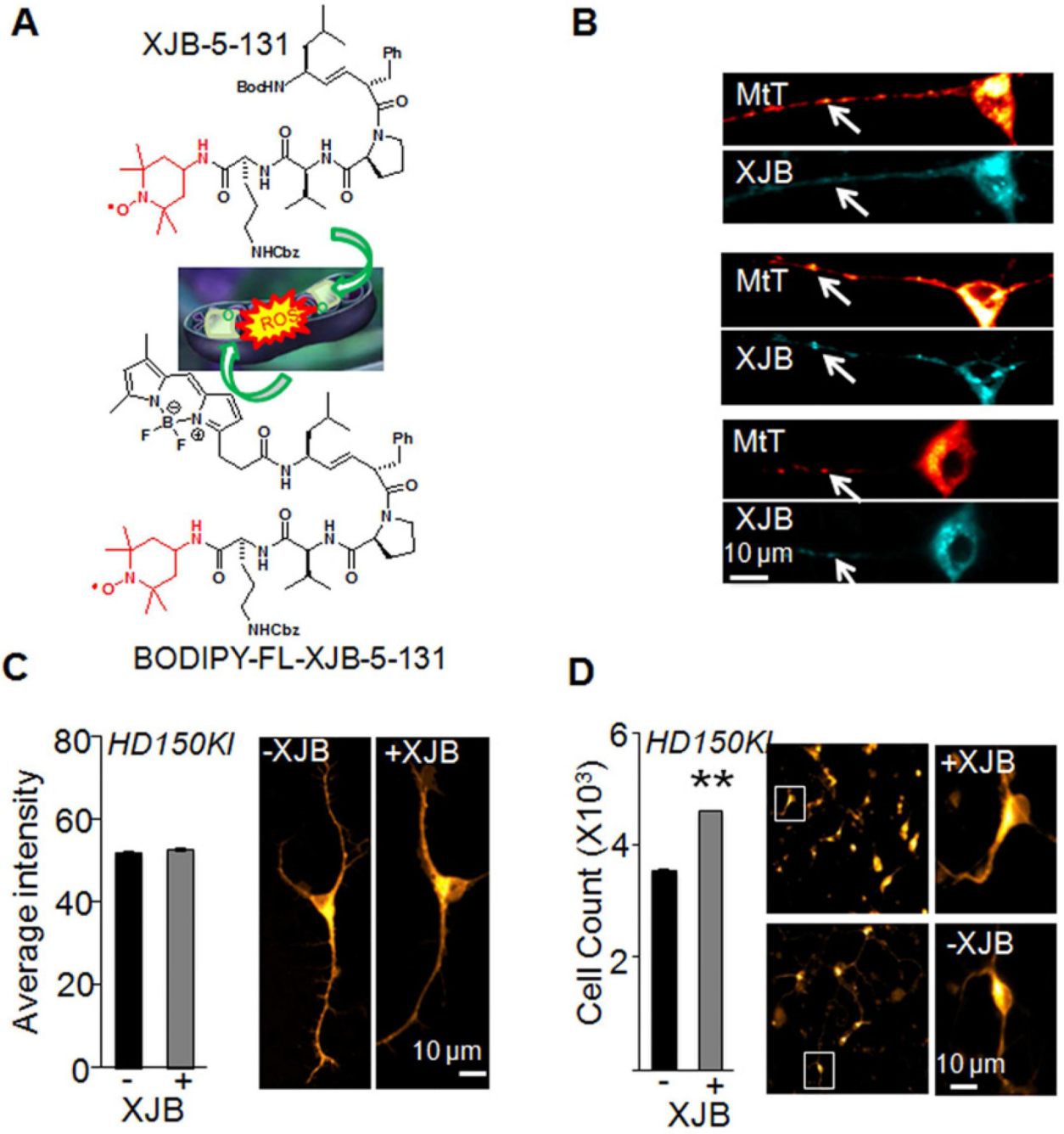

Figure 1. XJB-5-131 is localized to mitochondria (MT) and enhances neuronal survival in a mouse model of HD

(A) Schematic diagram of the structure and functional design of XJB-5-131 and BODIPY-fluorescent labeled (FL)-XJB-5-131. The structure in red is a stable nitroxide free-radical with reactive oxygen species (ROS) scavenging abilities. The structure in black is derived from a cyclopeptide antibiotic, gramicidin S, which selectively accumulates within microbial cell membranes. BODIPY-FL-XJB-5-131 was designed to validate its mitochondrial localization. **(B)** MitoTracker Deep Red (MtT, red) and BODIPY-FL-XJB-5-131 (XJB, cyan) co-label MT in primary striatal neurons from embryonic day 17 *HD150KI* mice. The arrowheads indicate representative MT detected by both probes. Scale

bar is 10 microns. **(C)** XJB-5-131 treatment (1 μM) for a week does not induce measureable changes in the number of MT in primary striatal neurons as quantified after staining with MitoTracker Deep Red intensity. The right panels are representative images. The total number of cells analyzed per condition is >10,000 from three independent experiments. Data are mean ± SEM (n = 3). Scale bar is 10 microns. (**D)** XJB-5-131 treatment protects survival of primary striatal neurons after 7 days in culture. The right panels are representative images. Scale bar is 10 microns. Data are mean ± SEM (n = 3). **, $P < 0.01$ using the unpaired two-tailed Student's t-test. XJB-5-131 is abbreviated as XJB in the figures. See also Figure S1.

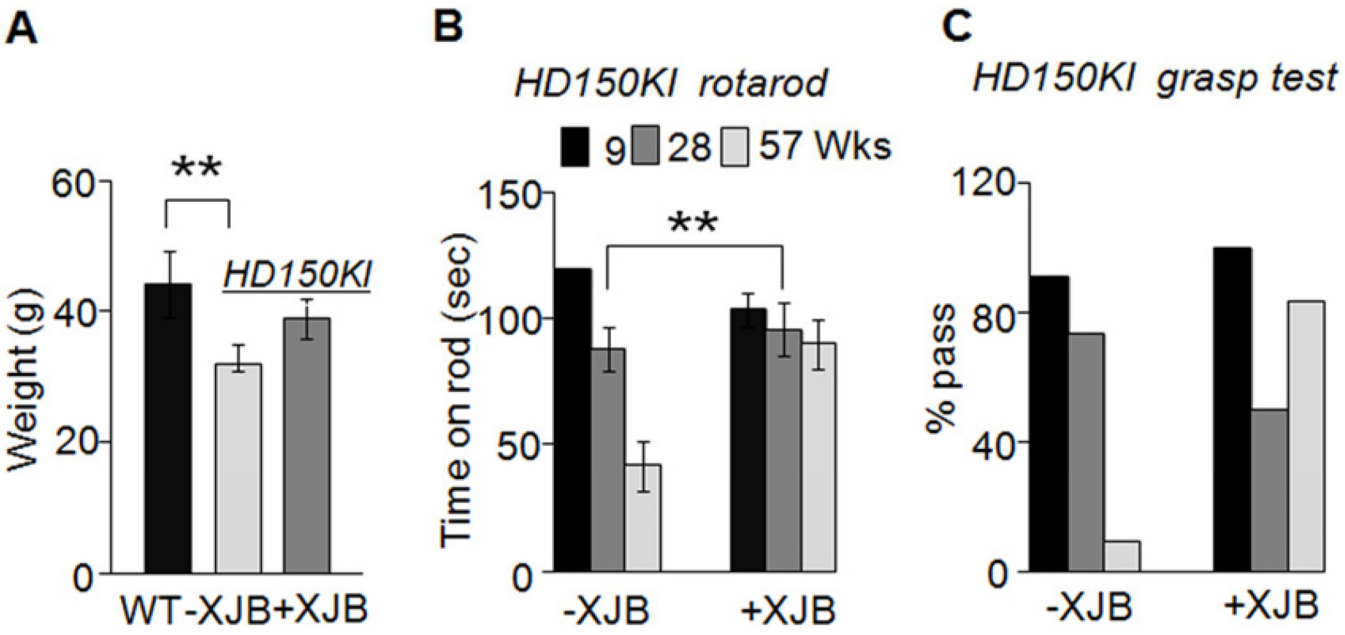

Figure 2. XJB-5-131 suppresses decline of weight loss and motor function in a mouse model of HD

(**A**) Weight of 57-week C57BL/6 wild-type (WT, n = 15), untreated *HD150KI* (− XJB, n= 7), and XJB-5-131-treated *HD150KI* (+ XJB, n = 10) mice. n is the number of mice used. Data are mean ± SEM, n = 7-15 mice/group. **, $P < 0.01$ using the unpaired two-tailed Student's t-test. (**B**) Rotarod performance and (**C**) grip strength test of animals at the age of 9, 28, and 57 weeks (Wks) with (+ XJB, n = 10) and without (−XJB, n = 7) XJB-5-131 treatment. Grasp test was deemed a pass if the animals held the bar for 30 seconds (within three trials). Each age group of animals was tested together and the results were expressed as % pass. n is the number of mice used. Data aremean ± SEM, n = 7-10. **, $P < 0.01$ using the unpaired two-tailed Student's t-test. XJB-5-131 is abbreviated as XJB in the figures.

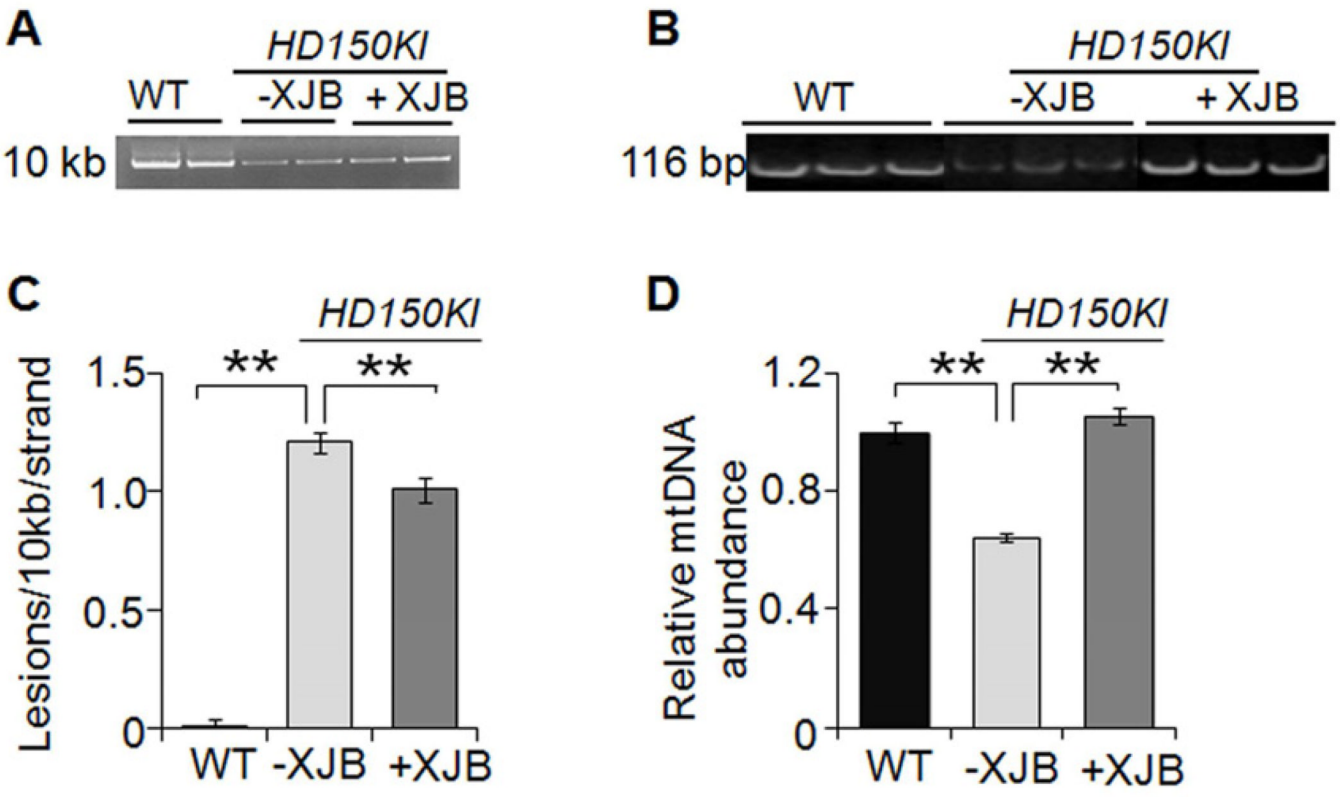

Figure 3. XJB-5-131 reduces mtDNA damage and maintains mtDNA copy number

(**A**) Representative agarose gel of the amplification of a 10 kb mtDNA fragment from WT, *HD150KI*, *HD150KI* + XJB-5-131 treated mice. (**B**) Representative agarose gel of the amplification of a 116 bp mtDNA fragment from WT, *HD150KI*, *HD150KI* + XJB-5-131 treated mice. (**C**) XJB-5-131 decreases the levels of mtDNA lesions in the cerebral cortex of *HD150KI* mice. Results were derived from three qPCR assays performed in duplicate on each animal. The number of mice used was 6, 7, and 6 for control, *HD150KI*, and *HD150KI* + XJB-5-131, respectively. Data are mean ± SEM (n = 6–7 mice/group). **, $P < 0.01$ using the unpaired two-tailed Student's t-test. (**D**) XJB-5-131 restores the abundance of mtDNA molecules in cerebral cortex of *HD150KI* mice. Results were derived from two qPCR assays performed in duplicate on each animal. The number of mice used was 6, 7, and 6 for control, *HD150KI*, and *HD150KI* + XJB-5-131, respectively. Data are mean ± SEM (n = 6–7 mice/group). **, $P < 0.01$ using the unpaired two-tailed Student's t-test. XJB-5-131 is abbreviated as XJB in the figures.

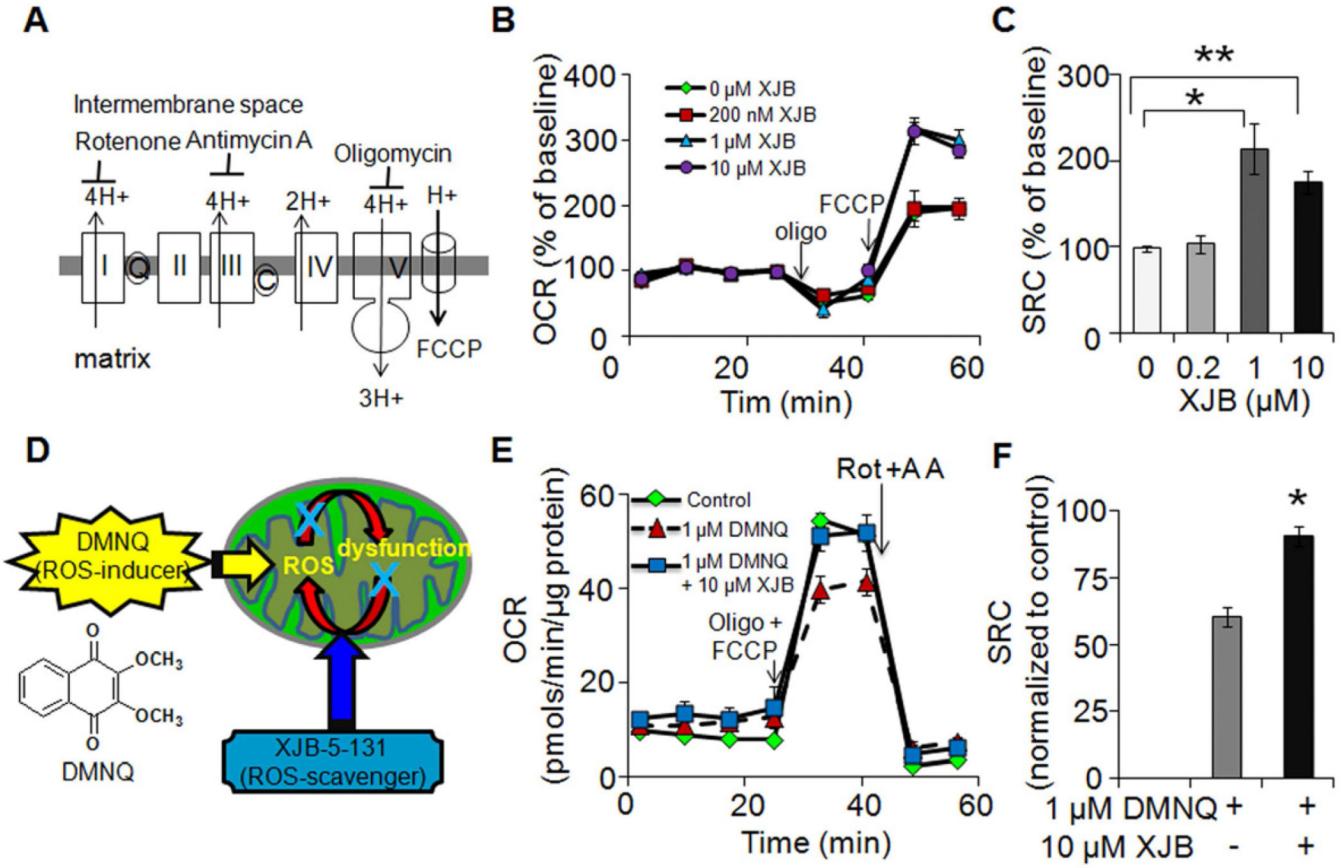

Figure 4. XJB-5-131 improves mitochondrial function in *HD150KI* animals

(A) Simplified diagram of electron transport chain and its inhibitors. Rotenone, antimycin A, and oligomycin are the inhibitors of Complex I, Complex III, and ATP synthase, respectively. Fluoro-carbonyl cyanide phenylhydrazone (FCCP) is an ionophore, which allows re-entry of the protons into the mitochondrial matrix and dissipates the proton gradient. **(B)** Representative profiles showing effects of XJB-5-131 treatment on oxygen consumption rates (OCR) under basal conditions and upon injections of mitochondrial inhibitors in isolated striatal synaptosomes from 57-week *HD150KI* mice. Each profile represents one independent biological experiment analyzed in triplicate. Data are means ± SEM (n = 3). The arrows indicate the injection of mitochondrial inhibitors. Three independent experiments were performed to obtain quantification of mitochondrial spare respiratory capacity (SRC) presented in (**C**). **(C)** Effects of XJB-5-131 treatment on SRC in isolated striatal synaptosomes. SRC is defined as the OCR difference between FCCP-induced respiration and basal respiration. Data represent three independent experiments and each was performed with five *HD150KI* mice and analyzed in triplicate. Data are mean ± SEM (n = 3). *$P < 0.05$, **, $P < 0.01$ using the unpaired two-tailed Student's t-test. **(D)** Schematic diagram illustrating the working hypothesis of DMNQ and XJB-5-131 within MT. **(E)** Representative profiles showing effects of DMNQ on OCR in the absence and presence of XJB-5-131 under basal conditions and upon injection of mitochondrial inhibitors. The down arrows indicate the injection of mitochondrial inhibitors. Each profile represents one independent biological experiment analyzed in triplicate. Data are means ± SEM (n = 3). Three independent experiments were performed to obtain quantification of mitochondrial SRC presented in (**F**). **(F)** XJB-5-131 treatment significantly improves mitochondrial SRC in 57-week *HD150KI* mouse striatal synaptosomes resulting from 1 μM

DMNQ exposure. Data are normalized to the control (in the absence of both XJB-5-131 and DMNQ) and are representative of three independent experiments. In each experiment, three *HD150KI* mice were used and analyzed in triplicate. Data are mean ± SEM (n = 3). *, $P < 0.05$ using the unpaired two-tailed Student's t-test. XJB-5-131 is abbreviated as XJB in the figures. See also Figure S2.